International Journal of Engineering Inventions
e-ISSN: 2278-7461, p-ISSN: 2319-6491
Volume 12, Issue 11 [November. 2023] PP: 61-81

The mechanical and microstructural characteristics of ultra-high-performance concrete (UHPC) made from industrial waste that is both economical and environmentally friendly

El Said Maaty. M. S. Elsharkawy, Marcos Youssef Lahzy
1,2Prof, Structural Engineering Dept., Faculty of Engineering, Tanta University, Tanta, Egypt
3MSc, Student, Faculty of Engineering, Tanta University, Tanta, Egypt

ABSTRACT: *The results and the effects of industrial waste on workability, mechanical characteristics, and microstructure features are covered in this study. The main goal of this research is to create sustainable UHPC mixtures by mixing environmentally favorable ingredients. This research investigates whether using different by-product materials to replace the spent PC partially could improve UHPC's sustainability. Industrial waste materials (IWM) such as ceramic waste powder (CWP), brick waste powder (BWP), and marble waste powder (MWP) were used in part lieu of PC in order to maintain a high degree of sustainability for UHPC. The inexpensive UHPC was made using CWP, BWP, and MWP at 5%, 10%, and up to 15% of the binder mass. In order to achieve a large working diameter and high strength UHPC, 15% silica fume was substituted for cement. The objective is to determine the highest sustainable material replacement rates at which UHPC can continue to perform at a very high level. Investigations were done on the microstructure, mechanical characteristics, and freshness of sustainable UHPC.*

KEYWORDS: *Ultra-high-performance concrete (UHPC), Industrial waste Compressive strength, Flexural strength, Microstructural performance*

Date of Submission: 09-11-2023 Date of acceptance: 23-11-2023

I. INTRODUCTION

Ordinary Portland Cement (OPC) production contributes to around 7-18% of worldwide carbon dioxide (CO2) emissions. One ton of OPC generated by calculations emits one ton of CO2 into the environment [1]. An expansion in OPC production to meet a huge concrete demand for infrastructure projects in certain densely populated nations would inevitably have a severe environmental effect. Furthermore, cement concrete's use as a construction material has increased steadily because of its in-situ flexibility, simplicity of use, durability, fire resistance, and great strength. However, OPC, one of the binders, is costly and pollutes the environment throughout production. It is well known that the production of OPC consumes a significant amount of energy while emitting a considerable amount of CO2 [1]. However, OPC remains the most commonly used binder in concrete, driving a hunt for more environmentally acceptable alternatives.

Conventional concrete (CC), also known as normal strength concrete [1], no longer satisfies the requirements for carrying out these works due to advancements in cement science and technology and the demand for thinner and bolder constructions. Then, to fill this demand, alternative concretes and cementitious mixes with superior qualities than CC evolved. High-strength concrete (HSC) [2], high-performance concrete (HPC) [1, 3], and, more recently, ultra-high-performance concrete (UHPC) [3, 4] all fall under this category. Due to the lack of technical standards that offer adequate definitions for these materials, it is widespread for these phrases to be used interchangeably. NBR 8953 [7], NBR 6118 [8], ACI 363 [9], ACI 318 [10], and BS EN 1992 [11] are a few standards for concrete constructions that distinguish between two classes of concrete based on characteristic compressive strength (fcu). For example, class I and Class II concrete have compressive strengths ranging from 20 to 50 MPa and 55 to 100 MPa, respectively. Class I concretes can be considered connected to the CC, whereas class II concretes are connected to the HSC.

While HPC and UHPC are defined in terms of performance, which considers workability, aesthetics, finish, integrity, durability, and mechanical strength, HSC is defined only in terms of compressive strength [12,13]. Although there is disagreement, a satisfactory definition for the HPC is that this concrete exhibit a workability comparable to self-compacting concrete (SCC), that is, a spread between 455 and 810 mm by the slump-flow test [1,14-16], but exhibits a compressive strength equivalent to the HSC, that is, fcu above 50 or 55 MPa [2,14]. Contrary to what is seen in ordinary concretes, where the water/binder factor (w/b) varies

from 0.45 to 0.65 [17-22], other writers propose that the w/b factor should be smaller than 0.40 [17–19]. When it comes to cement consumption, it often ranges from 400 to 700 kg/m3 [23–26], whereas for CC, it typically ranges from 260 to 380 kg/m3 [25–27,28].

On the other side, the UHPC has even more demanding standards. With a fluidity equal to or more than HPC and low porosity, some authors recommend a minimum strength of 120 MPa [13,29], while others call for a minimum of 150 MPa [30,31]. Theoretically, some concrete with strength above class II may have mechanical properties above those of HSC or HPC. In other words, the UHPC would fit into a strength class III made of these materials. The w/c ratio is between 0.2 and 0.3 [32,33] in conjunction with a very high cement consumption of around 800 to 1000 kg/m3 [34,35] to attain these qualities. Additionally, because UHPC is often made without including coarse particles, which would potentially transform it into mortar, the flow table test may be used to assess its workability. Without applying blows to the material, several writers advise that flow table measures be more than 260 mm [36].

UHPC is constructed from materials that are either expensive or include a lot of material, which boosts the cost of manufacturing and could prohibit UHPC from being employed more widely in the development sector [23]. Recent studies [24, 25] all noted that utilizing cement with unusually high cement contents would raise the hydration heat, cause exogenous shrinkages, and impact the total cost of the UHPC. This deficit must be filled by restoring a portion of the sizeable amount used for cement. The fresh and hardened characteristics of UHPCs may be significantly impacted, while expenses are also reduced by merging or consolidating SCMs. Cement and even silica fume must thus be replaced by pozzolanic materials such as FA, GBFS, industrial wastes (ceramic powder, marble powder, and brick powder), etc. By substituting these additional cementitious materials for a sizable portion of the PC that was used, the major significance requirement of sustainability will be satisfied [28]. It also serves an important and valuable purpose. SCMs might provide the raw materials required to produce UHPC, increasing demand and constricting supply [29]. However, according to Matte and Moranville [30], UHPC has a super thick microstructure, making it a material with excellent mechanical properties and astoundingly improved strength characteristics. This makes UHPC a material that is mainly impermeable. In addition to the previously mentioned superior properties, would the relatively small concrete sections produced by ultra-high-performance concrete compensate for the high production cost and the exorbitant prices of the materials used to make this type of concrete?

This research principally expects to create sustainable UHPC blends merging environmentally friendly materials. This study is essential to clarify the possibility of enhancing the sustainability of UHPC when using different by-product materials as a partial replacement for the used PC. Ceramic powder, marble powder, and brick powder were used as partial replacements for PC to maintain a tremendous degree of work on the sustainability of UHPC. Ceramic, marble, and brick powder were merged as 5% up to 20% from binder mass. SF has amounted to 15% of the absolute abundance of the employed cement. Another objective is to demonstrate the demonstration of high-quality mechanical properties of UHPC and to analyze the utilization of the better maintainable material kind and its ideal replacement percentage. The research aims to evaluate the mechanical and durability of ultra-high-performance concrete. The individual objectives will include.

1) Optimize the mix design for ultra-high-performance concrete with a target mean compressive strength greater than 120 MPa at 28 days.
2) Evaluation of the strength development of ultra-high performance concrete containing waste materials.
3) To study the durability properties of UHPC.
4) The feasibility and possibility of solid waste materials (SWM) incorporation in UHPC as a replacement for cement.
5) Using ceramic powder, marble powder, and brick powder as a partial replacement for Portland cement to produce UHPC.
6) The microstructure of UHPC was investigated.

II. EXPERIMENTAL SETUP

Portland cement is average (CEM I 52.5 N). The Lafarge Cement Company in Egypt provided the cement used in this investigation (LAFARGE). This cement meets BS EN 197-1/2011 requirements. According to E.S.S. No. 2421/2005, laboratory testing verified the cement's physical properties and chemical composition, indicating concrete work applicable in real-world scenarios. Water from a pure source was used in the mixing process. In every mixture, the water-to-binder ratio was 0.38. This experiment used ASTM C 1240-05 silica fume that has been densified and has a specific gravity of 2.29. High composite strength was attained by enhancing the cementitious ingredient in the mix with silica fume. The average particle size of silica fume was 13.0 μm. Low-calcium fly ash (Type F), having a specific gravity of 2.26, was utilized in this study.

which satisfies ASTM C 618 requirements. The Sika Company in Egypt supplied the fly ash used in this study. They were both obtained from Sika Corporation. The specific gravity of the natural sand is 2.56%. According to particle packing theory, the size of the natural sand particles determines optimal homogeneity.

Three industrial waste materials were used in this study as a partial cement substitute: ceramic waste powder (C.W.P.), brick waste powder (B.W.P.), and marble waste powder (M.W.P.). Chemical admixtures are frequently used to improve fresh and cured concrete properties. To improve the workability of the newly mixed concrete mixes and attain high strength for the produced concrete, a high-range water-reducing additive (superplasticizer) was employed.

The Sika ViscoCrete® 3425 superplasticizer, which has a modified polycarboxylate basis, was utilized in this study. The specific weight of the Viscocrete-3425 was 1.05.

Using the EMMA program and earlier research, which first established the material quantities and their particular weights, ultra-high-performance concrete mixes were produced. The best design approach was then investigated by calculating the total amount of all the portions. The combined ingredients of concrete mixes are displayed according to design. Table 1 show All ingredients combined.

.

CEM I	575 kg/m3-488 kg/m3
Sand	1150 kg/m3
Silica fume	210 kg/m3
Fly ash	260 kg/m3
Steel fiber	0%,1%and 2%
(Ceramic-Brick-Marble)	5%,10% and 15%

Table 1: All ingredients combined

Compressive strength

Before testing, the samples were taken from the curing tank and allowed to dry in the lab for roughly two hours. According to BS EN 12390-3:2019, the compressive strength has been measured 7, 28, and 90 days after casting. At each testing age, three specimen cubes (10*10*10 cm) from each mixture were examined, and the average was taken. The compressive test was conducted using a hydraulic testing machine in the Tanta University's College of Engineering laboratory.

Flexural strength

Flexural strength tests were performed on a plain beam at 7, 14, and 28 days. The flexural strength test was performed according to ASTM standards. The specimen was put on support blocks at the machine, and load-applying blocks were attached to it at one spot. During the test, the computer established and maintained a loading rate of 0.017 MPa/min with a sensitivity of 5 kN. When the fracture occurred in the middle third of the span length, the modulus of rupture or flexural strength could be determined (maximum bending moment area). The ultimate load was multiplied by the length and divided by geometrical parameters to calculate the flexural strength.

Young’s Modulus of Elasticity

UHPC was tested for 28 and 56 days on a cylinder sample. To compute Young's Modulus, the research used a stress-strain ratio and a lateral-to-longitudinal strain ratio of concrete. The ASTM values for Young's Modulus were obtained. Two strain-measuring devices, or LVDTs, were mounted to the cylinder to measure longitudinal strain. To quantify transverse strain, a third LVDT was mounted horizontally.

The sorptivity test

The sorptivity test was performed by the technique established by previous researchers [9], [10]. In line with ASTM C 1585-13, the rate of sorptivity of concrete samples was measured at 28 and 90 days. Separate solutions of 5% magnesium sulfate (MgSO4) and 5% sulphuric acid (H2SO4) were used to submerge the UHPC specimens. For up to 4 months, magnesium sulfate (MgSO4) by ASTM C1012-04 and sulfuric acid (H2SO4) by ASTM C267 were exposed. The solutions in the containers were changed every two weeks, and the compressive strength was tested constantly. Visual appearance, weight changes, and strength retentions assessed the effects of these chemicals on UHPC samples.

Non-Destructive Tests (Ultrasonic pulse velocity tester)

A 'Portable Ultrasonic Non-destructive Digital Indicating Tester' (PUNDIT) version 5 is used for finding the ultrasonic pulse velocity (UPV).

SEM/EDS Analysis

Scanning electron microscopy (SEM) is a kind of electron microscope that generates pictures by scanning a material with a focused electron beam. Following the interaction of these electrons with the sample's atoms, several signals are created that offer information on the compositional and topographic analyses of the sample. In a conventional SEM, the electron beam is emitted from an electron cannon attached to a tungsten filament (as a cathode) and electrically heated for electron emission owing to its highest melting point. In general, SEM samples may be scanned at high resolutions, even better than 1 nanometer. The general principle of SEM analysis is the detection of secondary electrons generated by sample atoms due to excitation by the electron beam. These secondary electrons are detected using a specific detector dependent on sample topography. After detecting secondary electrons, this detector presents a picture of the sample's surface topography.

X-ray diffraction (XRD)

X-ray diffraction (XRD) is used to identify the phases in a material (Figure 3.19). Diffraction is a physical phenomenon that occurs when electromagnetic waves escape barriers in their path. This phenomenon also applies in material science, where electromagnetic pulses such as X-rays are used to material atoms, and diffraction occurs as a reflection at certain angles. It operates on the premise that each crystalline phase has its diffraction picture.

Fourier Transform Infrared Spectral (FTIR) Analysis

The FTIR-8400S spectrum, SHIMADZU, Japan), was used to record the infrared absorption spectra of the geopolymer specimen samples. The spectra were collected in the wavelength region of 4000-400 cm-1 with 32 scans per spectrum.

III. RESULTS AND DISCUSSION

Compressive strength

Fig. 1 indicates the effects of steel fiber. Figs. 2,3, and 4 show the effects of industrial waste on the compressive strength (Fcu) of concrete that contains 2% steel fiber after 3, 7, 28, 56, and 90 days of curing. The compressive strength of normal UHPC was 102 MPa without steel fiber. With the addition of 1% steel fibers, the compressive strength of UHPC increased by 106 MPa. When the steel fiber content is 2%, the highest compressive strengths are obtained, which were 76.0, 86, 121, and 151.80 MPa at 3, 7, 28, and 90, respectively. The compressive strength of UHPC with 5% C.W.P. content can reach 111 MPa and 130.2 MPa at 28 and 56 days, respectively. This is a 14.1 and 13.4% reduction from the control mixture's values. It can be shown that UHPC's compressive strength increased with C.W.P. below 5%. This might be explained by the fact that C.W.P. with pozzolanic activity can interact with C.H. to encourage cement hydration and generate more CS-H gel. The compressive strength of UHPC increased with the increase in curing time, and at the same age, the compressive strength of UHPC increased with an increase in B.W.P. substitution amount of up to 10%. The 28-d strength of a 15% substitution rate can be reduced from 121 MPa to 112 MPa. The optimal M.W.P. content for UHPC specimens is a 10% replacement of Portland cement. The compressive strength at the optimal M.W.P. content increases by 7.5%, 7.77%, and 8.9%, respectively, compared to the control concrete at 3d, 7d, and 28d. [4,8,12,14,17]

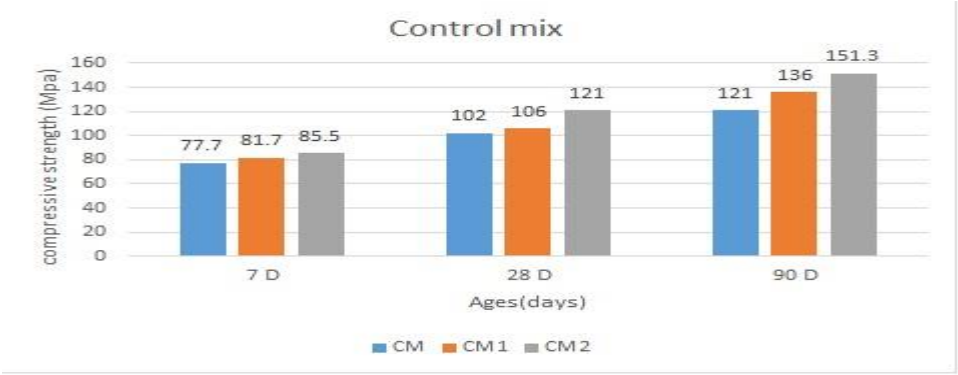

Figure 1 The steel fiber effect on compressive strength

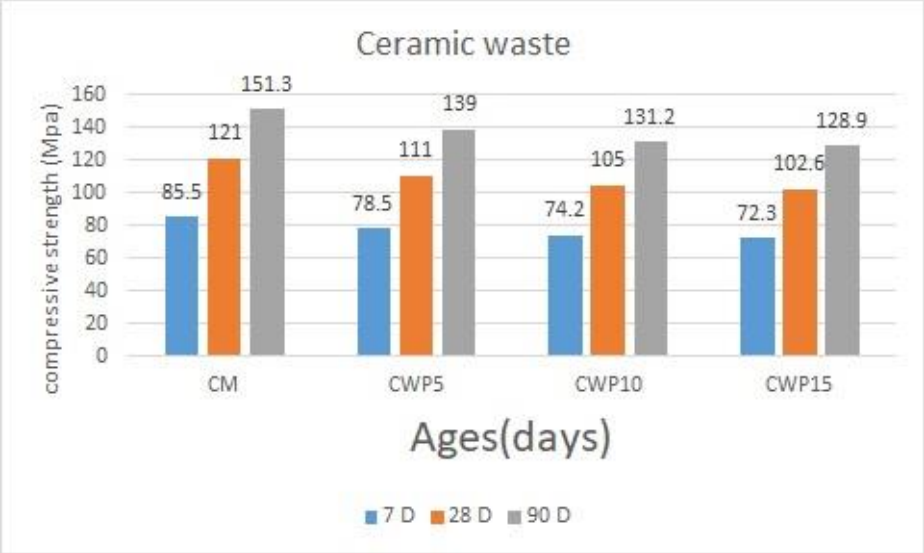

Figure 2 The ceramic effect on compressive strength

Figure 3 The Brick effect on compressive strength

Figure 4 The Marble effect on compressive strength

Elastic modulus

The relationship between the modulus of elasticity and compressive strength of UHPC with different waste materials is illustrated in Figures 5 and 6. When steel fiber content is increased, compressive strength and modulus of elasticity improve. The average compressive strength and elastic modulus of the reference mix (CM2) without steel fibers are 102.2 MPa and 33.1 GPa, respectively. The compressive strength and elastic modulus are 121.0 MPa and 38.9 GPa, respectively; when the steel fiber content is 2% [17], [31], [40], the addition of CWP results in a dramatic variation of the elastic modulus. Using 5%, 10%, and 15% of CWP as a cement replacement, the elastic modulus was 34.2, 33.1 and 32.3 GPa, respectively. Using 5%, 10%, and 15% of BWP as a cement replacement, the elastic modulus was 38.1, 39.2, and 37.3 GPa, respectively. Similarly, using 5%, 10%, and 15% of MWP as a replacement for cement, the elastic modulus was 33.2, 32.3, and 29.3 GPa, respectively. The divergence trend of compressive strength and elastic modulus is compatible with the previous studies on UHPC. The relationship between compressive strength and modulus of elasticity was matched with the empirical equation stated by [36]. Figure 4.12 presents the relation between the modulus of elasticity and compressive strength.

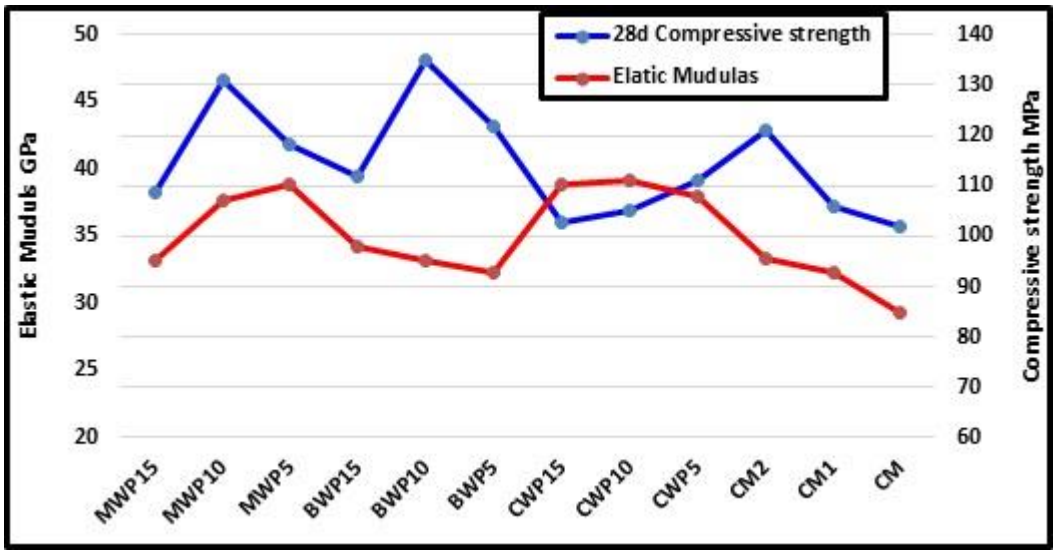

Figure 5 The relation between modulus of elasticity and compressive strength

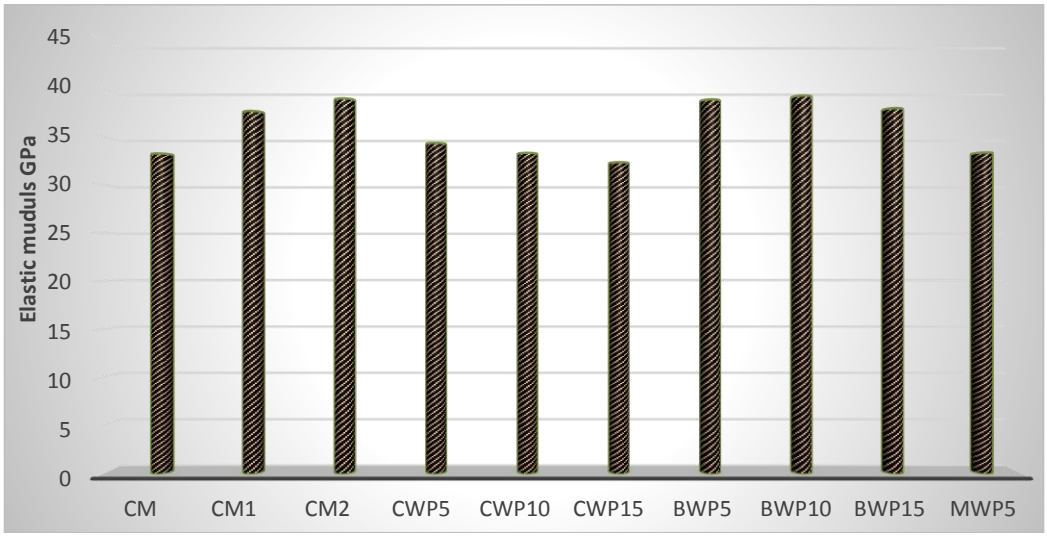

Figure 6 Modulus of elasticity of prepared UHPC**.**

Flexural strength

Figure 7 presents the flexural strength of UHPC samples. Flexural strength in UHPC was developed similarly to compressive strength. The lowest flexural strength of 7.96 MPa is achieved without adding steel fiber, while the highest strength of 10.90 MPa is achieved with a 2% steel fiber content. Chen et al. [17] noticed that increasing the steel fiber quantity significantly increases the flexural strength of UHPC.

Figure 8 shows the effect of ceramic waste powder on the flexural strength of the UHPC. The development of flexural strength of the prepared UHPC specimens with CWP at 28 days is illustrated in Figure 4.14. According to Figure 4.14, the optimal CWP regarding the tensile strength is the same as that regarding the compressive strength, which is 10%. When taking the tensile strength of CM2 as the standard, CWP should not exceed 15%. Besides, the growth in tensile strength compared to the control mixture is more significant than the growth in compressive strength. The possible reason is that the tensile strength of concrete is more sensitive to the changes in ITZ properties and in the pore, structure caused by different CWP content, which needs further exploration in future studies. Figure 9 displays the 28-day and 56-day UHPC strengths with various BWP contents. When PC is partially substituted with BWP, the UHPC mixture's mechanical properties are altered to variable degrees. The 3-day flexural strengths of BWP5, BWP10, and BWP15, respectively, are lower than those of CM2 by 14.04%, 6.34%, 18.3%, and 14.13%. This is primarily because BWP integration reduces the quantity of new hydration products in the UHPC mixture, which reduces the compactness of the microstructure [19]. However, because the packing state of the solid particles in UHPC considerably influences the strengths of the mixture, the relationship between compressive strength and BWP substitution ratio is not entirely evident. Compared to the sample (0% BWP), the 28-day compressive strength of the specimen with 15% BWP is reduced by 12.16%, while the improved value of the specimen with 13.1% BWP is raised by 4.81%. This might be connected to the modified packing density of the system. When the BWP particle size, which is between cement and SF, is present, the system reaches the ideal packing state. When low-activity BWP is used in place of cement, the mechanical characteristics of UHPC are reduced; nonetheless, the specimen containing 15% BWP has compressive strengths that are comparable to those of UHPC, with 28-day and 56-day compressive strengths that are 96.09% and 96.30% of UHPC, respectively. The impact of marble waste powder on the UHPC's splitting strength is depicted in Figure 10 shows the evolution of tensile strength of the prepared UHPC specimens with BWP at 28 days. Figure 9's impacts of BWP replacement can be used to make conclusions consistent with those in Figure 9. The ideal BWP for tensile strength, as shown in Figure 9, is 10%, also the best BWP for compressive strength. BWP shouldn't exceed 15% when using the tensile strength of CM2 as the benchmark. Additionally, the increase in compressive strength is less significant than the increase in tensile strength compared to the control combination. The potential cause, which will require further investigation in further experiments, is that the tensile strength of concrete is more sensitive to changes in ITZ characteristics and the pore structure produced by varying BWP concentrations. Finally, the relationship between flexural strength and compressive strength is shown in Figure 11.

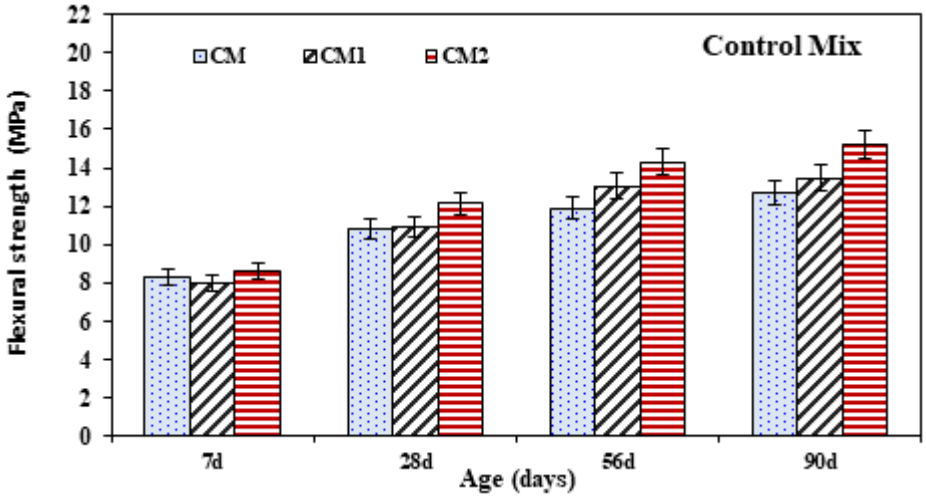

Figure 7 Effect of steel fiber on the flexural strength of UHPC.

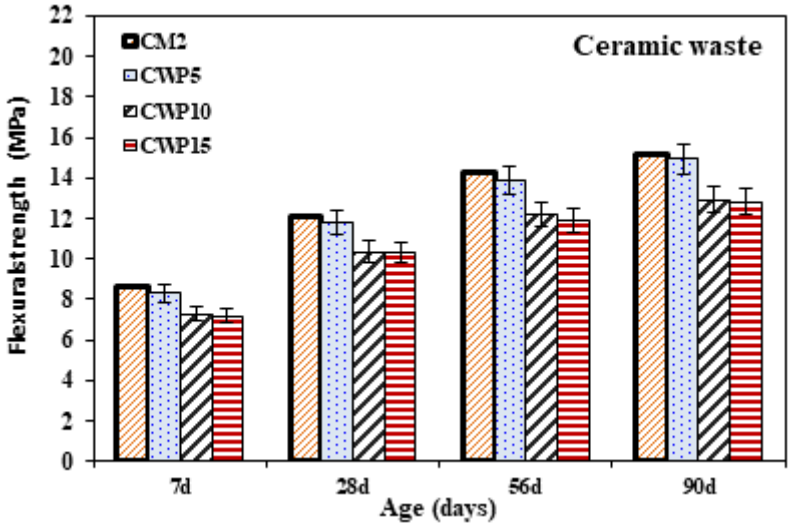

Figure 8 Effect of Ceramic waste on the flexural strength of UHPC.

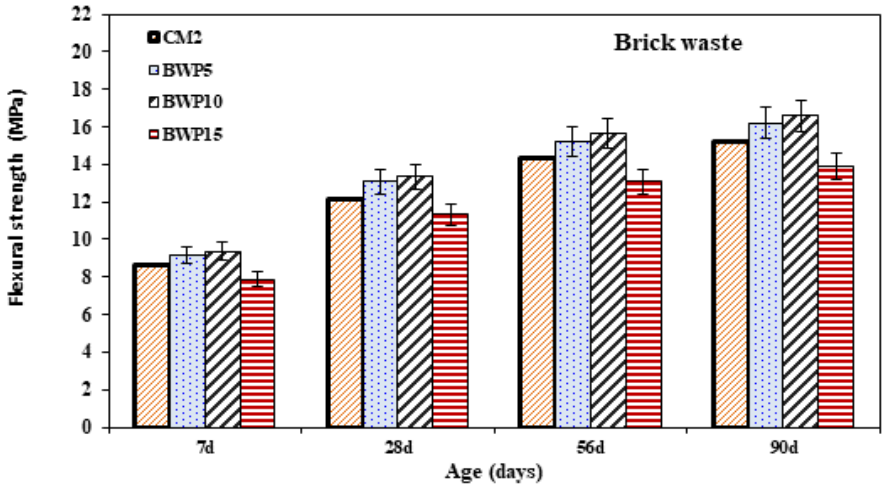

Figure 9 Effect of brick waste on the flexural strength of UHPC

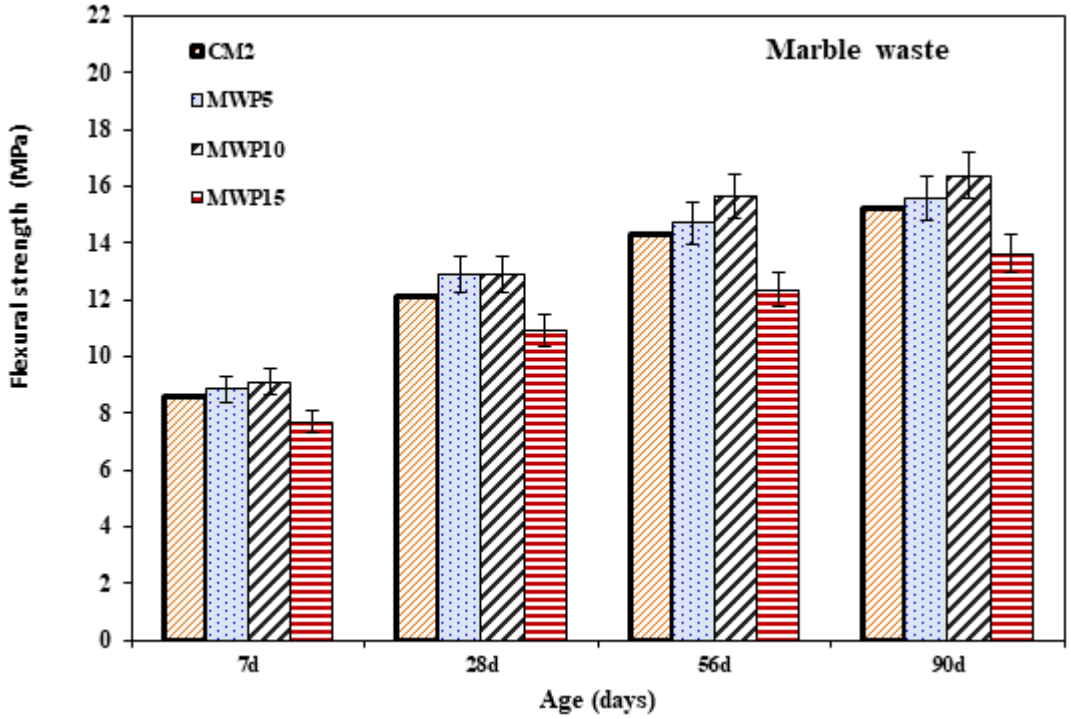

Figure 10 Effect of Marble waste on the flexural strength of UHPC.

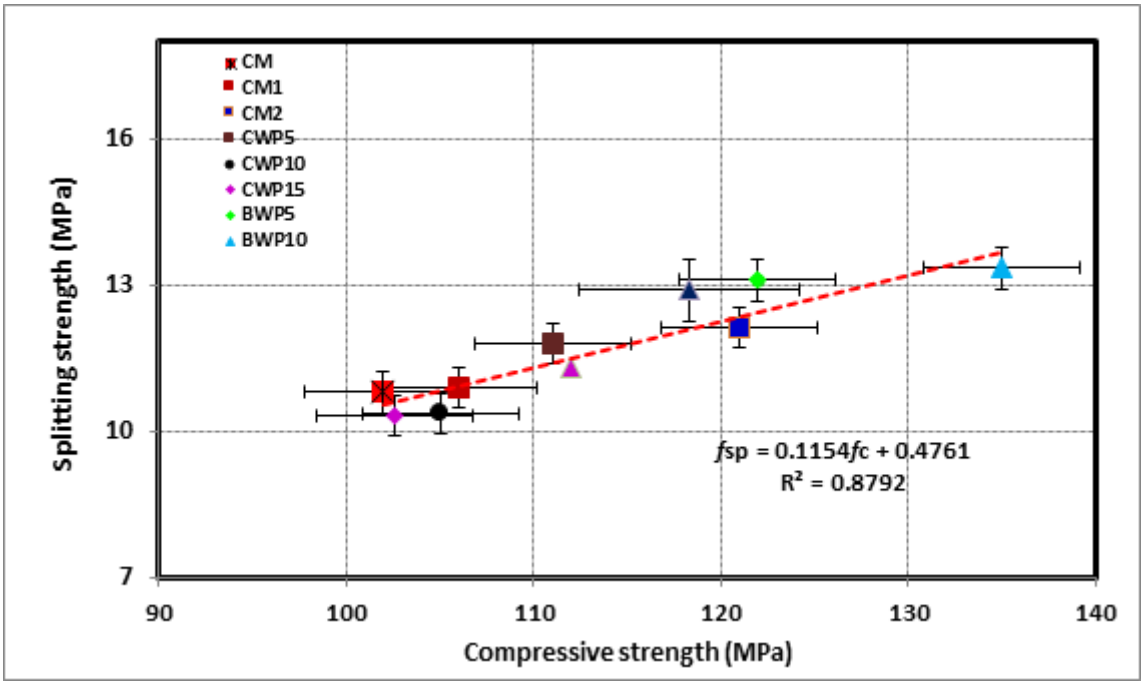

Figure 11 relation between the splitting and compressive strength of UHPC.

Ultrasonic Pulse Velocity Test Results (UPV)

To assess the strength of the developed UHPC, ultrasonic pulse velocity (UPV) was used as a non-destructive approach. [41], [42]. The experiment was conducted on dry concrete at 28 days, as shown in Figure 12 . It is clear from the recorded velocities that the UPV values increased with the inclusion of steel fiber. Compared to the control mixes with and without waste materials, the UPV of UHPC was lowered by around 6.49%. 6.9%, 8.65%, with the inclusion of 5%,10%, and 15% of CWP. Analogously, compared to the control mix with the inclusion of 5%,10%, and 15% of BWP, it resulted in an increase in UPV value at 10%, which was increased by 4.16 %. This occurred due to the decreased porosity of BWP-UHPC mixtures compared to the

control mix, as sound transmits through solid materials faster than through porous materials. The results obtained from the UPV agree with the compressive strength [43].

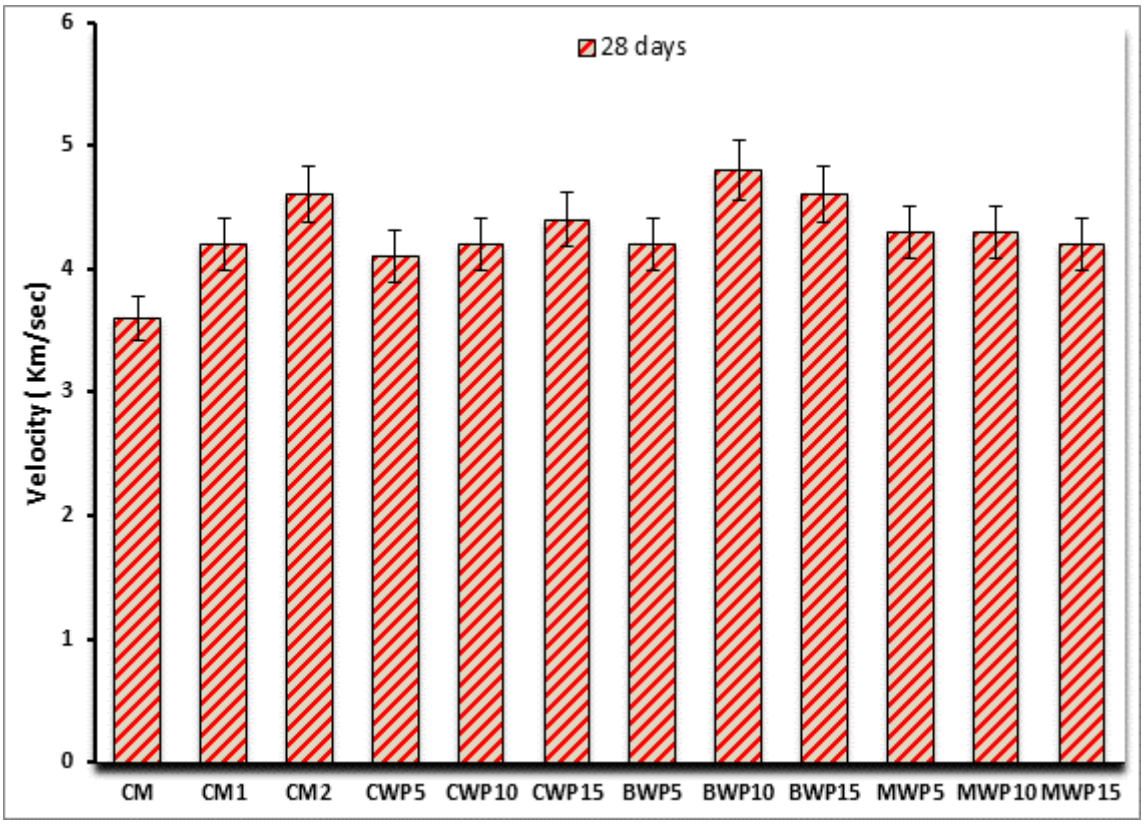

Figure 12 Results of UPV of UHPC mixtures at 28 days.

Water absorption

Figure 13 presents the results of the water absorption values of UHPC samples at 28 and 90 days. The lower average values, as evaluated on 3 specimens of each UHPC, were CM2 mixture, which was obtained at 2.29% and 2.69% at 28 and 90 days. The highest values were the BWP10 mixture (15% brick waste), which was received at 3.89% and 4.77% at 28 and 90 days. According to recent studies [18,22-26], active pozzolanic materials play an essential part in diminishing UHPC absorption; consequently, the degradation in absorption may be related to the reduction of the pores in the prepared mixtures or the disconnect of the linked pore network. Furthermore, the results obtained are consistent with the findings of Prem et al. [44], which examined effects in ternary cementitious systems.

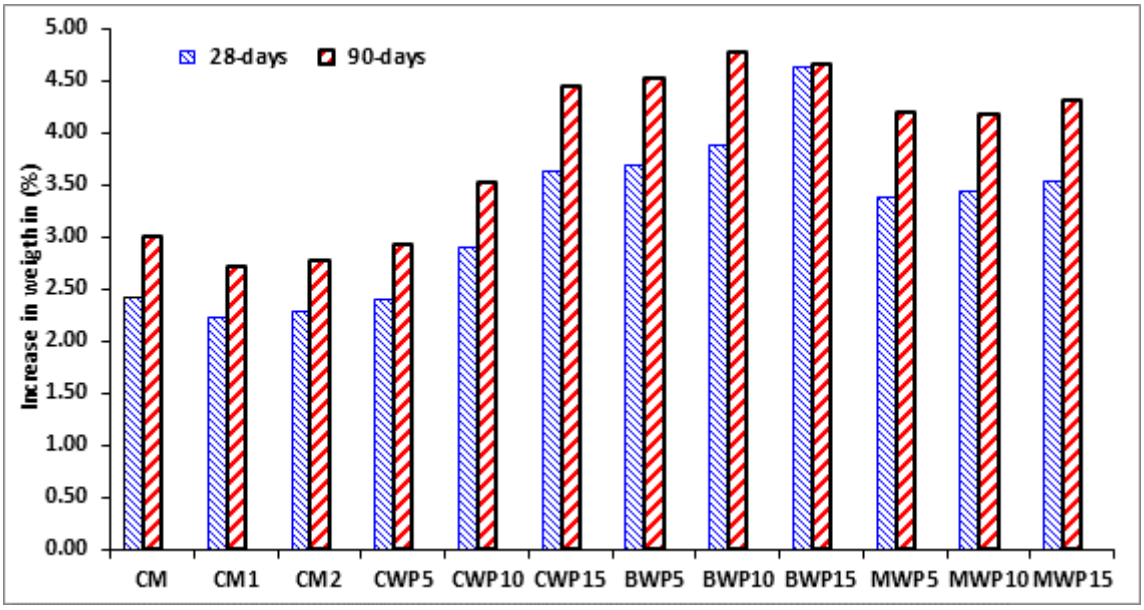

Figure 13 . Results of water absorption of UHPC mixtures at 28 days.

SEM Analysis

S.E.M. shows microstructure micrographs of the control mix of UHPC (CM2) samples after 28 days. It was seen in Figure (10-1) that the microstructure of the UHPC contains a few quantities of incompletely reacted, and a distributed number of unreacted cement nanoparticles, but the microstructure is generally thick and compressed. Figure (10-2) shows that the sample forms relatively dense hydration products, and the C.W.P. can also be found in the picture, uniformly distributed in the matrix.

It can be seen from the photo that hydration products adhere to and grow on the surface of C.W.P. With the increase of C.W.P. content, the number of "growth sites" also increases, which is conducive to the transfer and growth of hydration products. At the same time, the content of practical reaction components in cementitious materials is decreased by the increase of the C.W.P., which causes a decrease in the production of hydration products.

However, the content of hydration products is stable due to the decrease in the concentration of active components in the cementing material. The interaction of the two mechanisms results in the exact content of hydration products of the C.W.P.- UHPC with an appropriate amount of C.W.P., and the macroscopic properties are stable. The microcracks and micropores of UHPC were reduced compared to the control mixture. It indicates that the microstructure of UHPC becomes denser. The results of the influence of brick powder content on the microstructure of UHPC are prepared by replacing cement and analyzing the changes in the microstructure of the UHPC matrix when using optimum brick powder content. When 10% brick powder content is added, the structure is more compact, and the large proportion of amorphous SiO2 in the M.W.P. and the packing capability of the UHPC matrix may be attributed to the enhancement in the microstructure and properties of the UHPC. Several elements were exhibited, including

1-the excellent smoothness and spherical properties, which assisted in replacing the water caught between the fine and coarse particles

2 -The influence on the flow of the blend (reduces flow reluctance) as a well-dispersed multiphase system with an intensive microstructure and low permeability.

3-The interaction with calcium hydroxide led to the creation of an extra gel, which caused the result of a thick and strong C-S- H gel.(9,11,15)

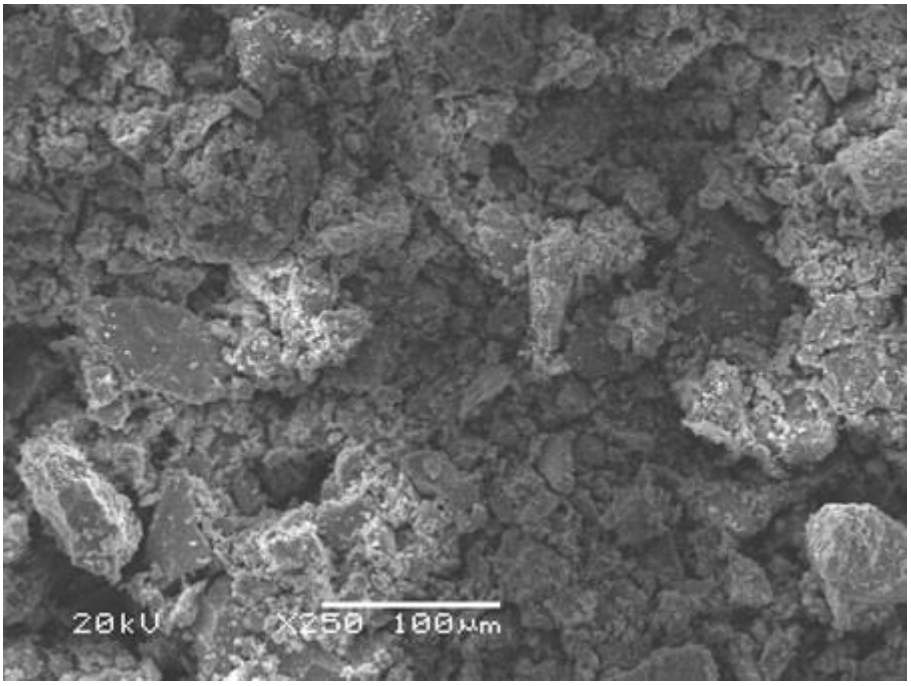

Figure 14 SEM for control mix

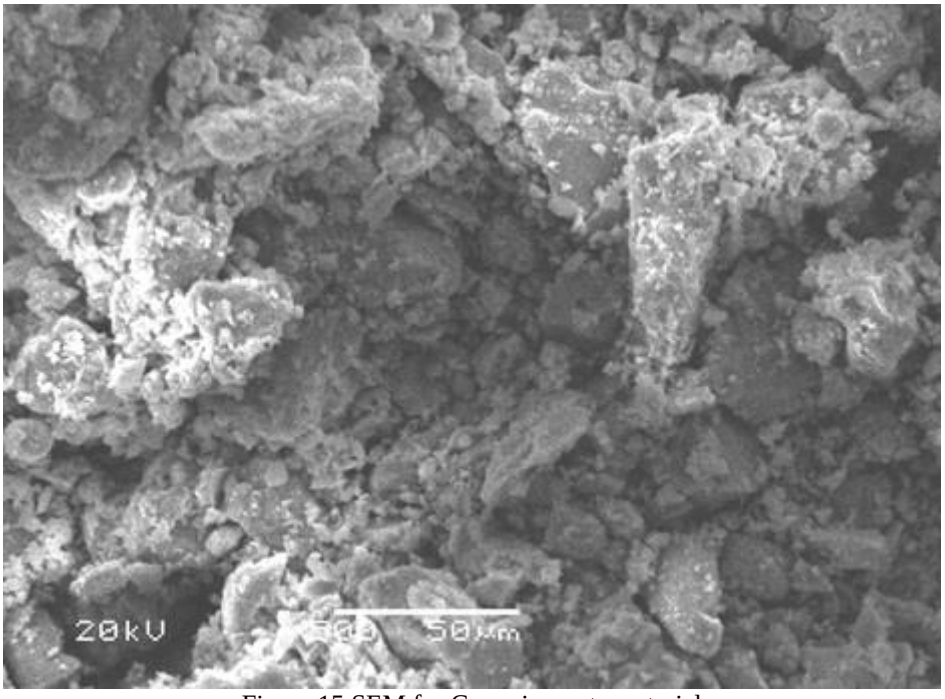

Figure 15 SEM for Ceramic waste material

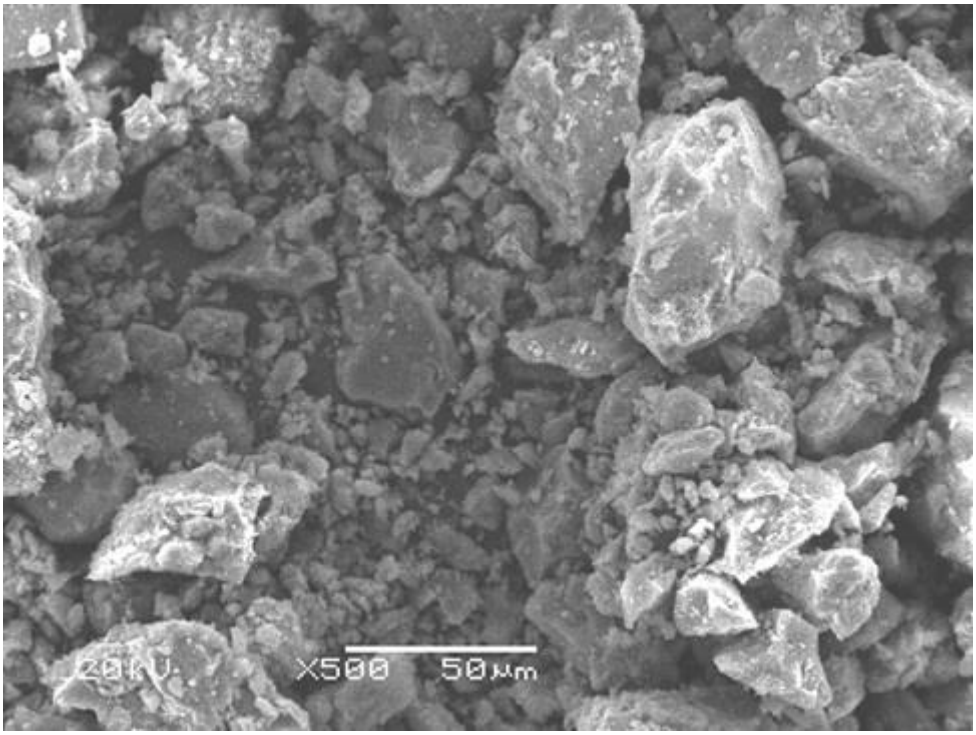

Figure 16 SEM for Brick waste material

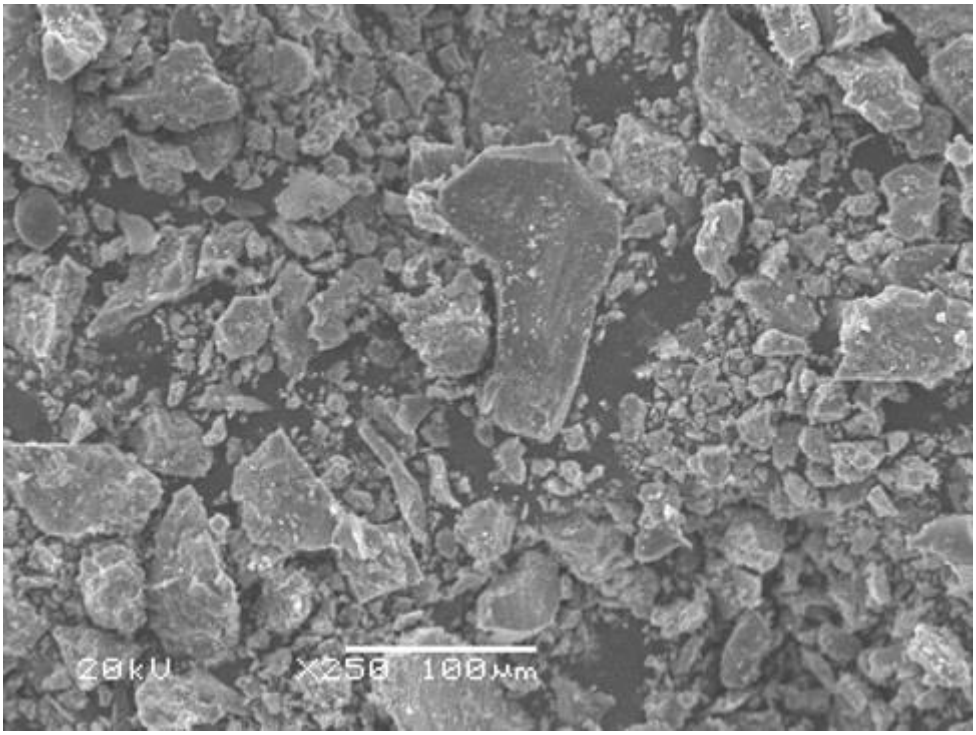

Figure 17 SEM for Marble waste material

X-ray diffraction (XRD)

Figures 18 to 21 show the XRD pattern of UHPC (control mix), UHPC containing ceramic waste (CWP10), UHPC containing ceramic waste (BWP10), and UHPC having ceramic waste (MWP10) at 28 days .

It is generally difficult to see ettringite in the XRD results of UHPC-containing waste materials, while the C-S-H and CH phases can be seen. The XRD analyses in Figure 19 reveal that clinker reacts with water to form C-S-H and Portlandite in specimens subjected to standard curing. Moreover, ettringite is observed in those subjected to standard curing regimes. However, no crystalline phase or tobermorite is observed [90, 91]. The XRD investigations of UHPC specimens containing ceramic powder are presented in Figure 5.10 and reveal

that, except for the crystal hydration products of Portlandite and Ettringite, none of the monocular-aluminate, hemicarbonate, or calcium monocarbo-aluminate are detected at the angles examined in the XRD profiles. This is due to the low amount of C3A in the cement type used in the studies cited [30, 45]. The significant difference in UHPC with and without ceramic powder is the presence of CaCO3 at the peaks of the UHPC XRD profile. The mechanical properties of UHPC can be enhanced by using brick waste with an optimal content (BWP10), according to earlier studies [36, 47]. Its microstructure has been studied to understand better how BWP affects the mechanical characteristics of UHPC (Figure 20). According to the XRD diagrams of the UHPC specimen, the amount of calcium hydroxide peaks in the mixture decreases as BWP is added. At an ideal brick waste content, almost all these peaks vanish and are replaced by peaks related to C2S, C3S, and C4AF, depending on the presence of unhydrated cement particles. The amount of C3S and C-S-H produced grows according to the observations obtained on the XRD profiles in the UHPC, which includes slag in the high percentages of cement replacement with BWP. Due to quality degradation, marble waste cannot usually be recycled into new products. However, due to the high silicon and calcium concentration in its powder, it can be used as a cement substitute in concrete mixtures, preventing waste from being dumped into the environment [101]. According to the XRD patterns of a UHPC microstructure shown in Figure 21, adding more marble powder causes UHPC to have a lower CH content as well as lower peak intensities of C2S and C3S, which suggests that marble powder and portlandite react to generate C-S-H. Marble powder is not as effective as a pozzolanic compound as cement, as evidenced by the significant drop in C2S + C3S but an increased reacted portlandite at high replacement levels. Additionally, it has been found that marble powder in UHPC exhibits an increase in its amorphous phase, which may be related to the improved C-S-H phase.

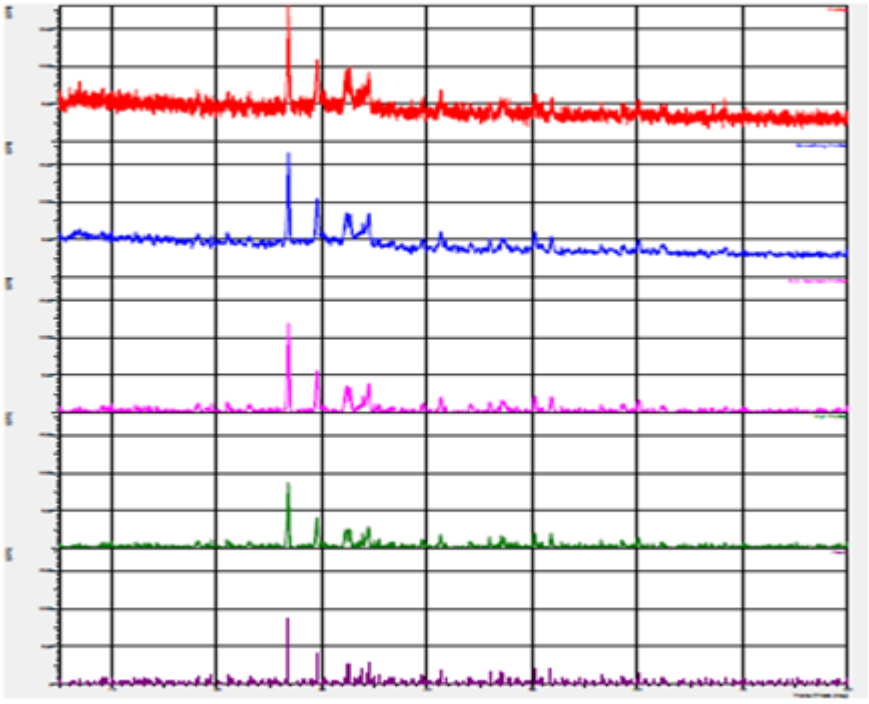

Figure. 18 XRD results of UHPC (Control Mix)

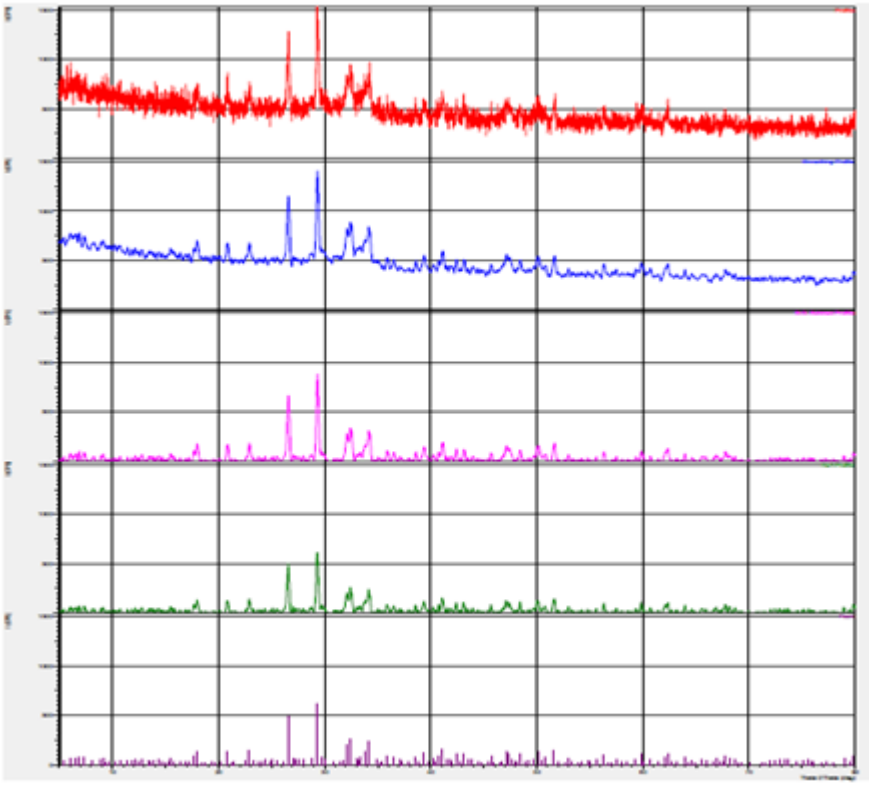

Figure. 19 XRD results of UHPC (CWP)

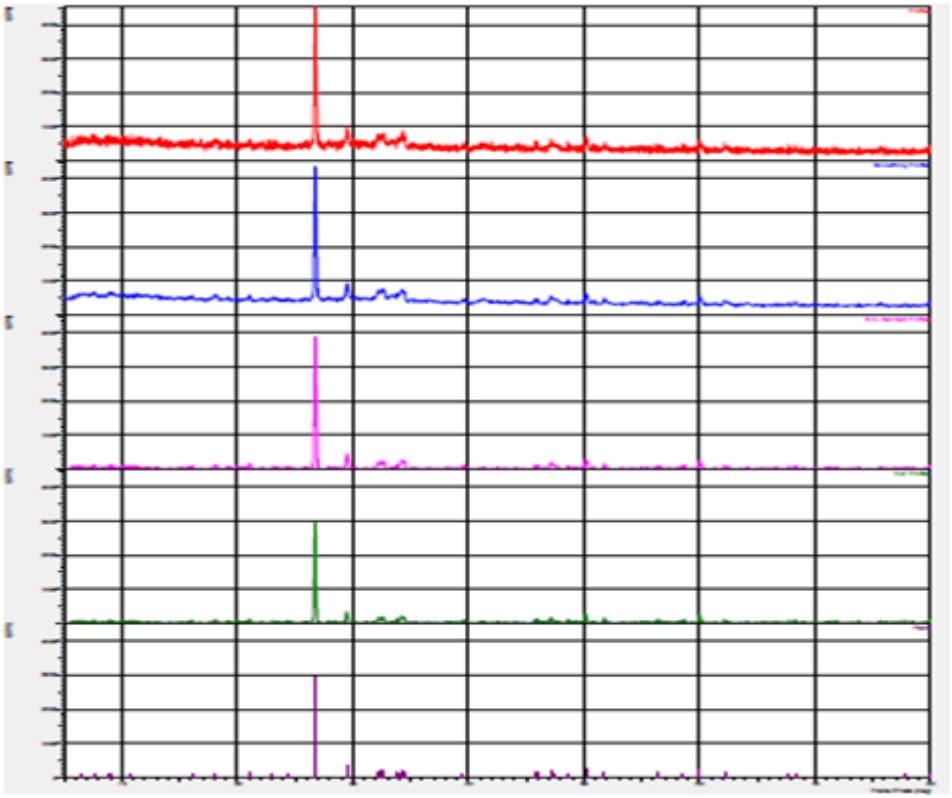

Figure. 20 XRD results of UHPC (BWP)

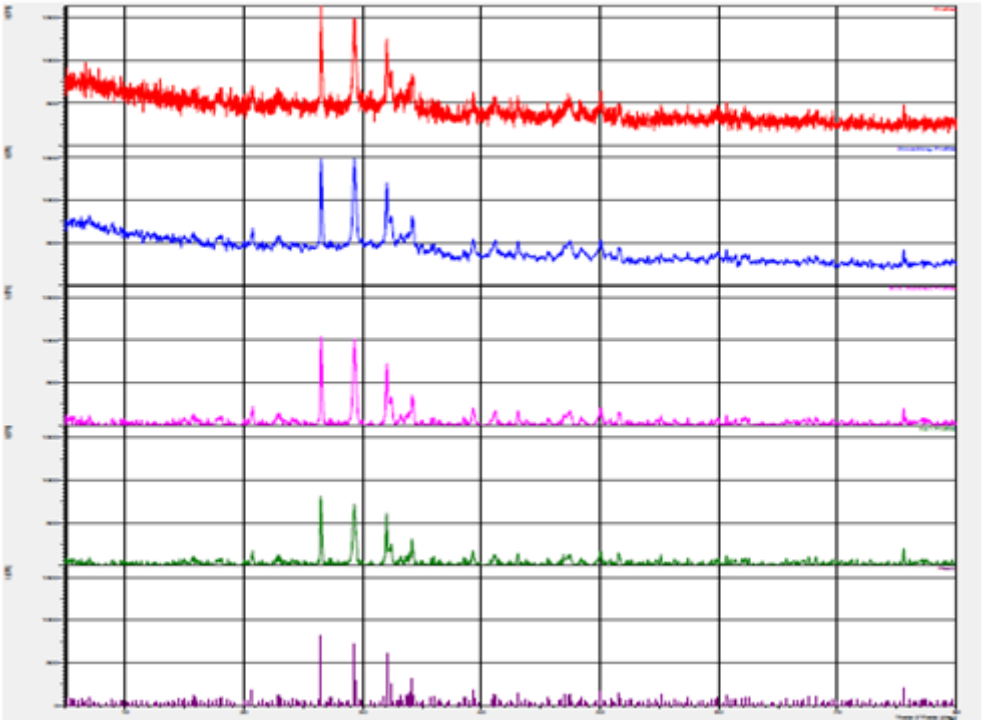

Figure. 21 XRD results of UHPC (MWP)

FTIR patterns (500–4000 cm−1) of 28-day standard-cured UHPC are depicted in Figures. 22 to 25. The UHPC-FTIR spectra of the samples with various waste material contents are shown in Figures. 22 to 25 after 28 days of cure. The O-H stretching vibration of Ca (OH)2 causes the absorption peak at 3644 cm1 [29]. The O-H bending vibration of C-S-H is represented by the peak at 1644 cm-1, the asymmetric stretching vibration at 1412 cm-1, and the symmetric stretching vibration is represented by the peak at 1066 cm-1. The out-of-plane bending vibrations of [33] correspond to the peaks at 875 and 711 cm-1. The asymmetric stretching and bending vibrations of Si-O are represented by the absorption peaks at 946 and 665 cm-1 correspondingly.[34]

The strength of the absorption peak (3644 cm1) corresponding to Ca(OH)2 is weak for all samples, as shown in Figure. 23. This agreed with the XRD findings. This demonstrates that most of the Ca(OH)2 generated by hydration after 28 days of curing was consumed by the ceramic, brick, and marble waste processes. Additionally, the intensities of all linked absorption peaks (1412, 1066, 875, and 711 cm1) dramatically increased as the dry ice content rose. From 5% to 10% of brick powder, the gain impact became more pronounced. This shows that adding brick powder encourages CaCO3 formation and is essential for cleaning the pores. Additionally, when the quantity of brick powder rose, the intensity of the absorption peak at 1644 cm-1 steadily increased. This demonstrates that including brick powder e encourages the development of C-S-H gels.

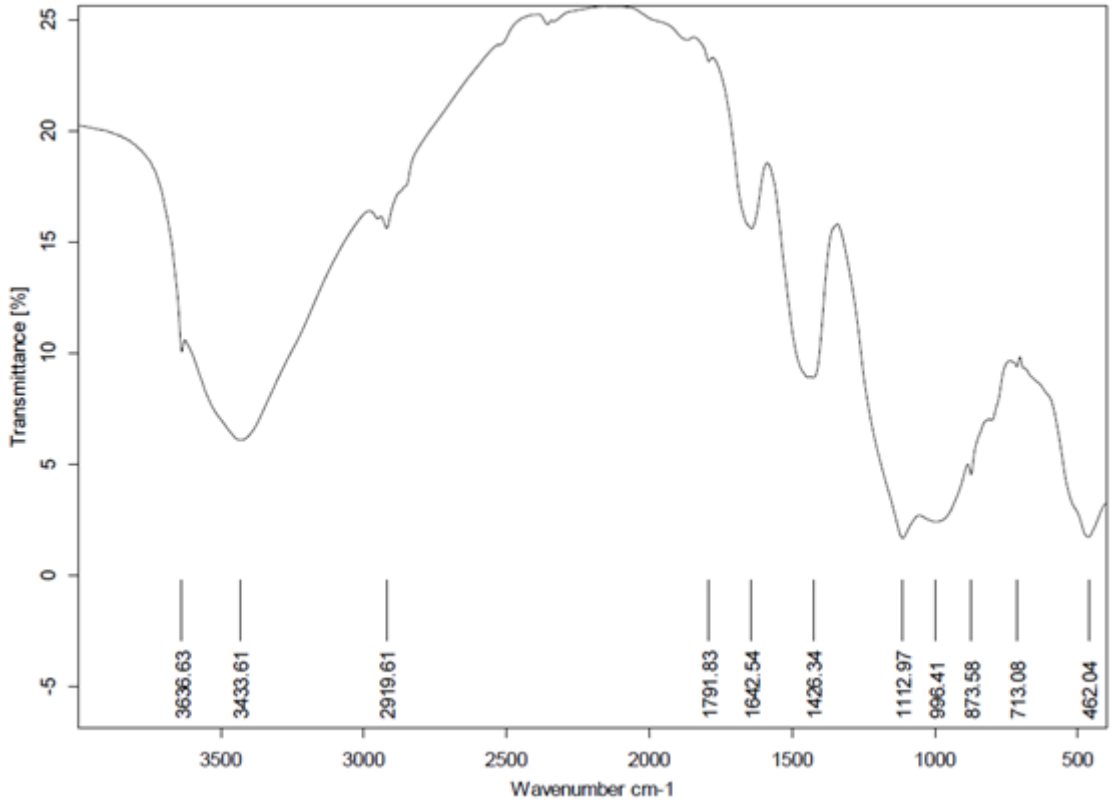

Figure. 22 FT-IR results of UHPC (Control Mix)

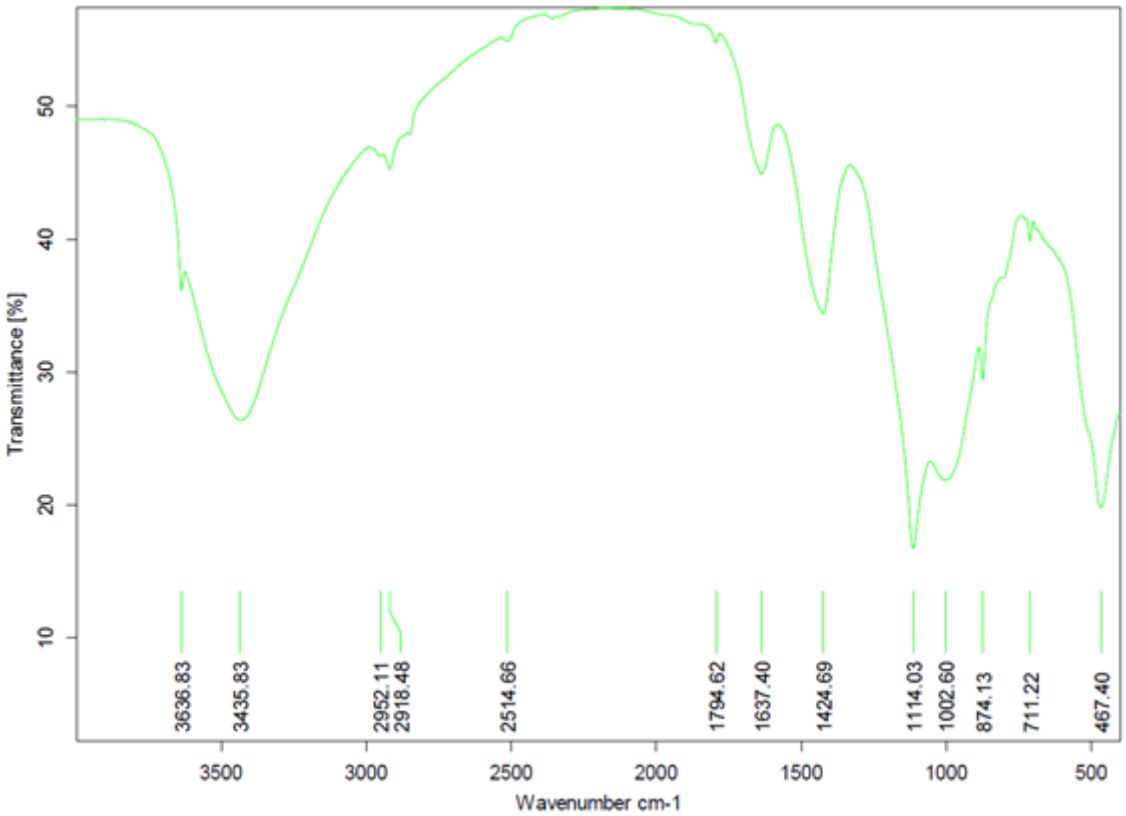

Figure 23 FT-IR results of UHPC (CWP)

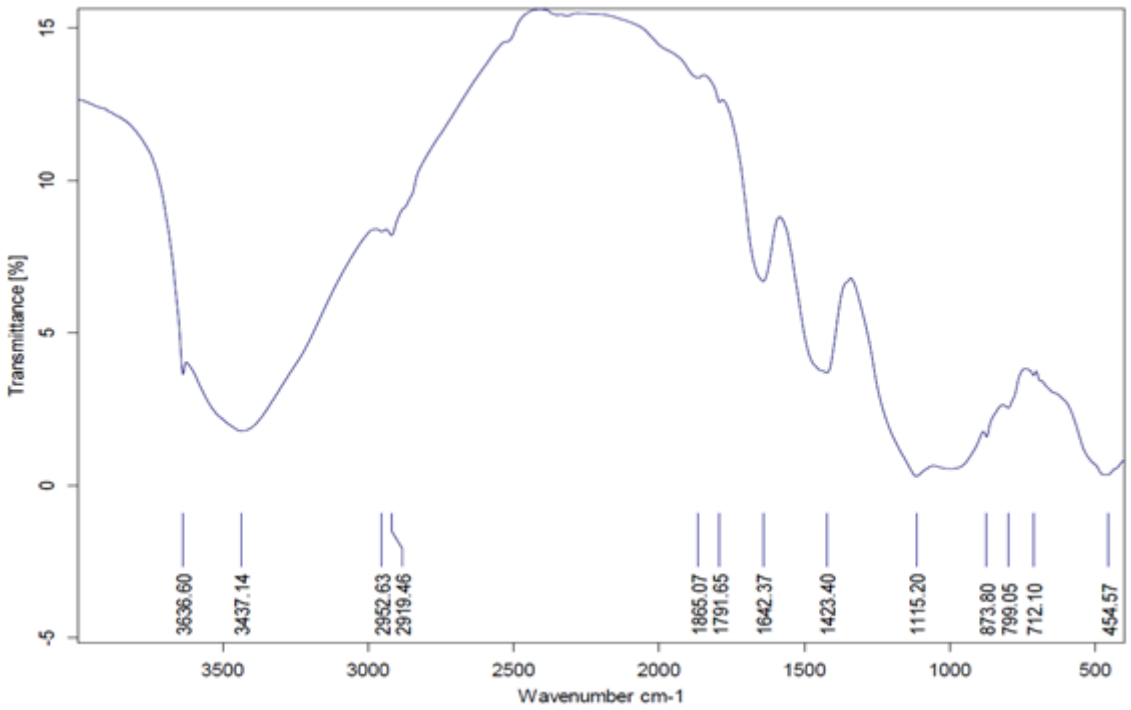

Figure. 24 FT-IR results of UHPC (BWP)

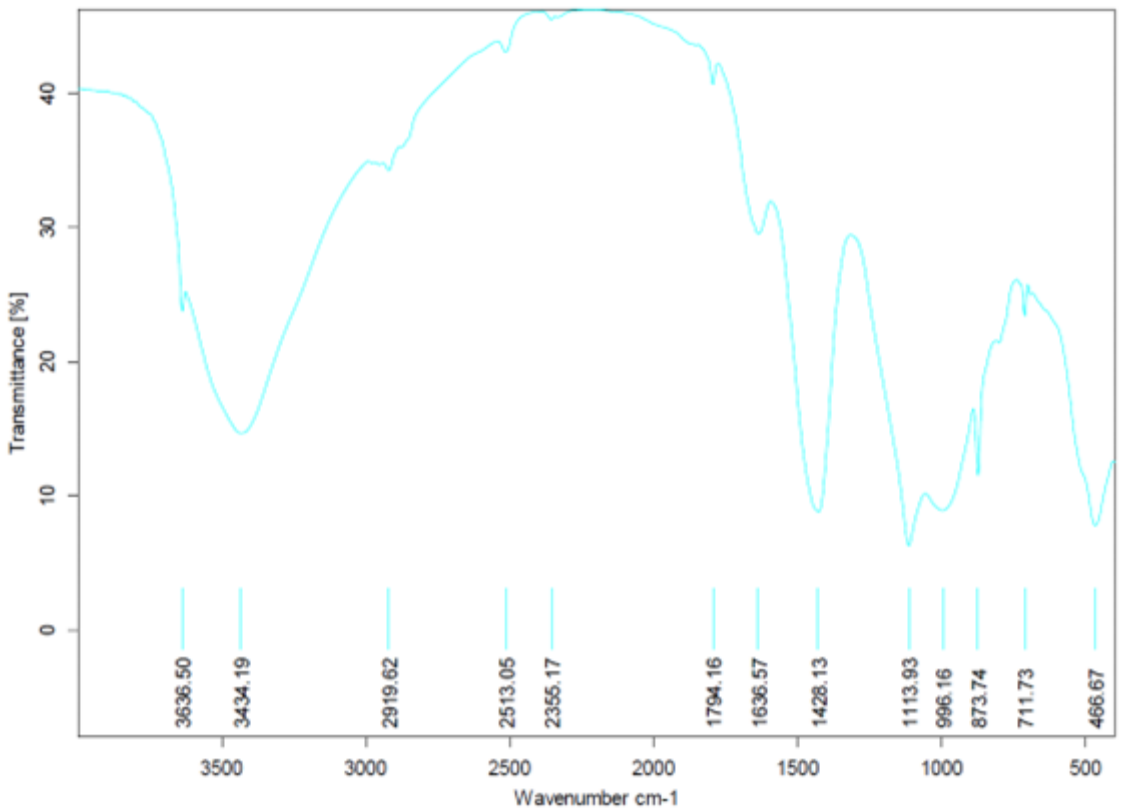

Figure. 25 FT-IR results of UHPC (MWP)

IV. CONCLUSION

The following conclusions were extracted from the accomplished experimental tests:

1. Compared to the control mixes with and without waste materials, the UPV of UHPC was lowered by around 6.49%. 6.9%, 8.65%, with the inclusion of 5%,10%, and 15% of CWP. Analogously, compared to the control mix with the inclusion of 5%,10%, and 15% of BWP, it resulted in an increase in UPV value at 10%, which was increased by 4.16 %. This occurred due to the decreased porosity of BWP-UHPC mixtures compared to the control mix, as sound transmits through solid materials faster than through porous materials.
2. The average values of water absorption of the control mixture were obtained at 2.29% and 2.69% at 28 and 90 days. The water absorption values increased with brick waste content, which was obtained at 3.89% and 4.77% at 28 and 90 days.
3. SEM photographs of the morphology of the UHPC samples indicate a high-density microstructure with relatively few capillary holes, particularly when 5% marble powder is added, and these SEM findings confirmed the mechanical properties results.
4. The UHPC-FTIR spectra of the samples with various waste material contents after 28 days of cure were investigated. The O-H stretching vibration of Ca (OH)2 causes the absorption peak at 3644 cm-1. The O-H bending vibration of C-S-H for ceramic waste samples is represented by the peak at 1644 cm-1, and the peak represents the asymmetric stretching vibration at 1412 cm-1. The gain impact became more pronounced from 10% of brick powder samples. This shows that adding brick powder encourages CaCO3 formation and is essential for cleaning the pores. The O-H bending for marble waste samples is represented by the peak at 2335 cm-1, and the peak represents the asymmetric stretching vibration at 2513 cm-1.

V. Recommendations For Future Work

1-Study the performance of ultra-high-performance concrete under the exposure of spalling.

2-Study the use of other eco-friendly replacement materials, such as recycled agricultural wastes in ultra-high-performance concrete mixtures.

3-Studying the behavior of ultra-high-performance concrete under the influence of different impact loads by changing the type and content of the added fibers and the used aggregates

4-Investigate the performance of UHPC with waste materials members constructed in the field compared to conventional UHPC members.

5- Study the utilization of nanoparticles such as nano-silica, nano clay, or carbon nanotubes in the production of UHPGC.

REFERENCES

[1]. Y. Dong, 'Performance assessment and design of ultra-high-performance concrete (UHPC) structures incorporating life-cycle cost and environmental impacts', Constr. Build. Mater., vol.167, 2018, doi: 10.1016/j.conbuildmat.2018.02.037.

[2]. P. Zhan, J. Xu, J. Wang, and C. Jiang, 'Multi-scale study on synergistic effect of cement replacement by metakaolin and typical supplementary cementitious materials on properties of ultra-high-performance concrete', Constr. Build. Mater., vol.307,2021, doi: https://doi.org/10.1016/j.conbuildmat.2021.125082.

[3]. Ç. Yalçınkaya and O. Çopuroğlu, 'Hydration heat, strength and microstructure characteristics of UHPC containing blast furnace slag', J. Build. Eng., vol.34, 2021, doi: 10.1016/j.jobe.2020.101915.

[4]. A. S. Faried, S. A. Mostafa, B. A. Tayeh, and T. A. Tawfik, 'Mechanical and durability properties of ultra-high-performance concrete incorporated with various nano waste materials under different curing conditions', J. Build. Eng., vol. 43,2021, doi: 10.1016/j.jobe.2021.102569.

[5]. D. Qian et al., 'A novel development of green ultra-high-performance concrete (UHPC) based on appropriate application of recycled cementitious material', J. Clean. Prod., vol. 261, 2020, doi: 10.1016/j.jclepro.2020.121231.

[6]. H. Zhang, T. Ji, B. He, and L. He, 'Performance of ultra-high-performance concrete (UHPC) with cement partially replaced by ground granite powder (GGP) under different curing conditions', Constr. Build. Mater., vol. 213,2019, doi: 10.1016/j.conbuildmat.2019.04.058.

[7]. Y. Shi, G. Long, C. Ma, Y. Xie, and J. He, 'Design and preparation of ultra-high-performance concrete with low environmental impact', J. Clean. Prod., vol. 214,2019, doi: 10.1016/j.jclepro.2018.12.318.

[8]. A. A. Abadel, M. I. Khan, and R. Masmoudi, 'Experimental and numerical study of compressive behavior of axially loaded circular ultra-high-performance concrete-filled tube columns', Case Stud. Constr. Mater., vol. 17, 2022, doi: https://doi.org/10.1016/j.cscm.2022.e01376

[9]. C. Shi, Z. Wu, J. Xiao, D. Wang, Z. Huang, and Z. Fang, 'A review on ultra-high-performance concrete: Part I. Raw materials and mixture design', Constr. Build. Mater., vol. 101, 2015, doi: 10.1016/j.conbuildmat.2015.10.088.

[10]. A. M. Tahwia, G. M. Elgendy, and M. Amin, 'Mechanical properties of affordable and sustainable ultra-high-performance concrete', vol. 16, 2022.

[11]. A. M. Tahwia, M. Abd Ellatief, A. M. Heneigel, and M. Abd Elrahman, 'Characteristics of eco-friendly ultra-high performance geopolymer concrete incorporating waste materials', Ceram. Int., vol. 48(14),2022, doi: https://doi.org/10.1016/j.ceramint.2022.03.103.

[12]. I. Y. Hakeem, M. Amin, A. M. Zeyad, B. A. Tayeh, A. M. Maglad, and I. S. Agwa, 'Effects of nano sized sesame stalk and rice straw ashes on high-strength concrete properties', J.Clean.Prod., vol.370,2022, doi: https://doi.org/10.1016/j.jclepro.2022.133542.

[13]. Hermann, C., & Kara, S. (Eds.), 'Sustainable Production, Life Cycle Engineering and Management'. Springer, 2012.

[14]. A. M. Tahwia, Ashraf Heniegal, Mohamed S. Elgamal, Bassam A. Tayeh. 'The prediction of compressive strength and non-destructive tests of sustainable concrete by using artificial neural networks'. Computers and Concrete, An International Journal, 27(1),2021, DOI: https://doi.org/10.12989/cac.2021.27.1.000.

[15]. R. Yu, Q. Song, X. Wang, Z. Zhang, Z. Shui, and H. J. H. Brouwers, 'Sustainable development of Ultra-High Performance Fibre Reinforced Concrete (UHPFRC): Towards to an optimized concrete matrix and efficient fibre application', J. Clean. Prod., vol. 162, 2017, doi: 10.1016/j.jclepro.2017.06.017.

[16]. M. Amin, A. M. Zeyad, B. A. Tayeh, I. Saad Agwa, and I. Saad, 'Effect of ferrosilicon and silica fume on mechanical, durability, and microstructure characteristics of ultra-high-performance concrete', Constr. Build. Mater., vol. 320, 2022, doi: 10.1016/j.conbuildmat.2021.126233.

[17]. R. Yu, P. Spiesz, and H. J. H. Brouwers, 'Effect of nano-silica on the hydration and microstructure development of Ultra-High-Performance Concrete (UHPC) with a low binder amount', Constr. Build. Mater., vol. 65, 2014, doi: 10.1016/j.conbuildmat.2014.04.063.

[18]. A. M. Tahwia, G. M. Elgendy, and M. Amin, 'Durability and microstructure of eco-efficient ultra-high-performance concrete', Constr. Build. Mater., vol.303, 2021, doi: 10.1016/j.conbuildmat.2021.124491.

[19]. A. Tafraoui, G. Escadeillas, S. Lebaili, and T. Vidal, 'Metakaolin in the formulation of UHPC', Constr. Build. Mater., vol. 23, 2009, doi: 10.1016/j.conbuildmat.2008.02.018.

[20]. Y. R. Alharbi, A. A. Abadel, O. A. Mayhoub, and M. Kohail, 'Effect of using available metakaolin and nano materials on the behavior of reactive powder concrete', Constr. Build. Mater., vol. 269, 2021, doi: https://doi.org/10.1016/j.conbuildmat.2020.121344

[21]. N. S. Ha, S. S. Marundrury, T. M. Pham, E. Pournasiri, F. Shi, and H. Hao, 'Effect of grounded blast furnace slag and rice husk ash on performance of ultra-high-performance concrete (UHPC) subjected to impact loading', Constr. Build. Mater., vol.329, 2022, doi: 10.1016/j.conbuildmat.2022.127213.

[22]. K. Wille, A. E. Naaman, S. El-Tawil, and G. J. Parra-Montesinos, 'Ultra-high-performance concrete and fiber reinforced concrete: Achieving strength and ductility without heat curing', Mater. Struct. Constr., vol. 45(3), 2012, doi: 10.1617/s11527-011-9767-0.

[23]. P. Shen, L. Lu, Y. He, F. Wang, and S. Hu, 'The effect of curing regimes on the mechanical properties, nano-mechanical properties and microstructure of ultra-high-performance concrete', Cem. Concr. Res., vol.118, 2019, doi: 10.1016/j.cemconres.2019.01.004.

[24]. J. F. Burroughs, J. Weiss, and J. E. Haddock, 'Influence of high volumes of silica fume on the rheological behavior of oil well cement pastes', Constr. Build. Mater., vol.203, 2019, doi: 10.1016/j.conbuildmat.2019.01.027.

[25]. P. P. Li, Y. Y. Y. Cao, H. J. H. Brouwers, W. Chen, and Q. L. Yu, 'Development and properties evaluation of sustainable ultra-high performance pastes with quaternaryblends',J.Clean.Prod.,vol.240, 2019, doi:10.1016/j.jclepro.2019.118124.

[26]. M. A. Mosaberpanah and O. Eren, 'Effect of quartz powder, quartz sand and water curing regimes on mechanical properties of UHPC using response surface modelling', Adv. Concr. Constr., vol.5(5),2017, doi:https://doi.org/10.12989/acc.2017.5.5.481.

[27]. EN, BS. Cement-Part 1: Composition, specifications, and conformity criteria for common cements (2011). British European Standards Specifications. EN BS.

[28]. D. Fan et al., 'A new development of eco-friendly Ultra-High-performance concrete (UHPC): Towards efficient steel slag application and multi-objective optimization', Constr.Build. Mater., vol.306,2021, doi: https://doi.org/10.1016/j.conbuildmat.2021.124913.

[29]. ASTM C494/C494M-17, 'Standard specification for silica fume used in cementitious mixtures. ASTM International, 2017.

[30]. ASTM C143/C143M-15a, 'Standard Test Method for Slump of Hydraulic-Cement Concrete'. ASTM International, 2015.

[31]. ASTM C1609/C1609M-12, 'Standard Test Method for Flexural Performance of Fiber-Reinforced Concrete (Using Beam with Third-Point Loading)'. ASTM International, 2012.

[32]. ASTM C39/C39M-17. 'Standard Test Method for Compressive Strength of Cylindrical Concrete Specimens'. ASTM International, 2017.

[33]. ASTM C496/C496M-17, 'Standard Test Method for Splitting Tensile Strength of Cylindrical Concrete Specimens'. ASTM International, 2017.

[34]. ASTM C1585-13, 'Standard Test Method for Measurement of Rate of Absorption of Water by Hydraulic-Cement Concretes'. ASTM International, 2017.

[35]. ASTM C494/C494M-17, 'Standard Test Method for Electrical Indication of Concrete's Ability to Resist Chloride Ion Penetration'. ASTM International, 2017.

[36]. S. Editors, C. Herrmann, and S. Kara, Sustainable Production, Life Cycle Engineering and Management Progress in Life Cycle Assessment. 2018.

[37]. Klöpffer, Walter, and Birgit Grahl. 'Life cycle assessment (LCA): a guide to best practice'. John Wiley & Sons, 2014.

[38]. A. M. Yousef, A. M. Tahwia, and N. A. Marami, 'Minimum shear reinforcement for ultra-high-performance fiber reinforced concrete deep beams', Constr. Build. Mater., vol.184, 2018, doi: https://doi.org/10.1016/j.conbuildmat.2018.06.022.

[39]. J. Du, Z. Liu, C. Christodoulatos, M. Conway, Y. Bao, and W. Meng, 'Utilization of off-specification fly ash in preparing ultra-high-performance concrete (UHPC): Mixture design, characterization, and life-cycle assessment', Resour. Conserv. Recycl., vol.180, 2022, doi: https://doi.org/10.1016/j.resconrec.2021.106136.

[40]. M. S. M. Norhasri, M. S. Hamidah, and A. M. Fadzil, 'Inclusion of nano metaclayed as additive in ultra-high-performance concrete (UHPC)', Constr. Build. Mater., vol.201, 2019, doi: 10.1016/j.conbuildmat.2019.01.006.

[41]. E. R. Teixeira, A. Camões, F. G. Branco, J. B. Aguiar, and R. Fangueiro, 'Recycling of biomass and coal fly ash as cement replacement material and its effect on hydration and carbonation of concrete', Waste Manag., vol. 94,2019, doi: 10.1016/j.wasman.2019.05.044.

[42]. X. Wang, D. Wu, J. Zhang, R. Yu, D. Hou, and Z. Shui, 'Design of sustainable ultra-high-performance concrete: A review', Constr. Build. Mater., vol.307,2021, doi: https://doi.org/10.1016/j.conbuildmat.2021.124643.

[43]. B. Zhang, T. Ji, Y. Ma, and Q. Zhang, 'Effect of metakaolin and magnesium oxide on flexural strength of ultra-high-performance concrete', Cem. Concr. Compos., vol. 131, p. 104582, 2022, doi: https://doi.org/10.1016/j.cemconcomp.2022.104582.

[44]. M. G. Sohail, R. Kahraman, N. Al Nuaimi, B. Gencturk, and W. Alnahhal, 'Durability characteristics of high and ultra-high-performance concretes', J. Build. Eng., vol. 33, p. 101669, 2021, doi: https://doi.org/10.1016/j.jobe.2020.101669.

[45]. M. J. Mohd Faizal, M. S. Hamidah, M. S. Muhd Norhasri, I. Noorli, and M. P. Mohamad Ezad Hafez, 'Chloride Permeability of Nanoclayed Ultra-High Performance Concrete BT - InCIEC 2014', 2015, pp. 613–623.

[46]. P. R. Prem, M. Verma, and P. S. Ambily, 'Sustainable cleaner production of concrete with high volume copper slag', J. Clean. Prod., vol. 193, pp. 43–58, 2018, doi: 10.1016/j.jclepro.2018.04.245.

[47]. S. Erdem, A. R. Dawson, and N. H. Thom, 'Impact load-induced micro-structural damage and micro-structure associated mechanical response of concrete made with different surface roughness and porosity aggregates', Cem. Concr. Res., vol. 42, no. 2, pp. 291–305, 2012, doi: https://doi.org/10.1016/j.cemconres.2011.09.015.
[48]. M. Amin, B. A. Tayeh, and I. S. Agwa, 'Effect of using mineral admixtures and ceramic wastes as coarse aggregates on properties of ultrahigh-performance concrete', J. Clean. Prod., vol. 273, p. 123073, 2020, doi: https://doi.org/10.1016/j.jclepro.2020.123073.
[49]. A. M. Tahwia, O. El-Far, and M. Amin, 'Characteristics of sustainable high strength concrete incorporating eco-friendly materials', Innov. Infrastruct. Solut., vol. 7, no. 1, pp. 1–13, 2022, doi: 10.1007/s41062-021-00609-7.
[50]. J. Du et al., 'New development of ultra-high-performance concrete (UHPC)', Compos. Part B Eng., vol. 224, p. 109220, 2021, doi: https://doi.org/10.1016/j.compositesb.2021.109220.
[51]. R. Jing, Y. Liu, and P. Yan, 'Uncovering the effect of fly ash cenospheres on the macroscopic properties and microstructure of ultra-high-performance concrete (UHPC)', Constr. Build. Mater., vol. 286, p. 122977, 2021, doi: 10.1016/j.conbuildmat.2021.122977.
[52]. J. Liu, C. Shi, and Z. Wu, 'Hardening, microstructure, and shrinkage development of UHPC: A review', J. Asian Concr. Fed., vol. 5, no. 2, pp. 1–19, 2019, doi: 10.18702/acf.2019.12.5.2.1.
[53]. O. M. Abdulkareem, A. Ben Fraj, M. Bouasker, L. Khouchaf, and A. Khelidj, 'Microstructural investigation of slag-blended UHPC: The effects of slag content and chemical/thermal activation', Constr. Build. Mater., vol. 292, p. 123455, 2021, doi: 10.1016/j.conbuildmat.2021.123455.
[54]. W. Lun Lam, P. Shen, Y. Cai, Y. Sun, Y. Zhang, and C. Sun Poon, 'Effects of seawater on UHPC: Macro and microstructure properties', Constr. Build. Mater., vol. 340, no. December 2021, p. 127767, 2022, doi: 10.1016/j.conbuildmat.2022.127767.
[55]. Z. Mo, X. Gao, and A. Su, 'Mechanical performances and microstructures of metakaolin contained UHPC matrix under steam curing conditions', Constr. Build. Mater., vol. 268, no. xxxx, p. 121112, 2021, doi: 10.1016/j.conbuildmat.2020.121112.